

Influence of the Morphology on the Functionalization of Graphene Nanoplatelets Analyzed by Comparative Photoelectron Spectroscopy with Soft and Hard X-Rays

Giovanni Chemello, Xenia Knigge, Dmitri Ciornii, Benjamin P. Reed, Andrew J. Pollard, Charles A. Clifford, Tom Howe, Neil Vyas, Vasile-Dan Hodoroaba, and Jörg Radnik*

Since its isolation, graphene has received growing attention from academia and industry due to its unique properties. However, the “what is my material” barrier hinders further commercialization. X-ray photoelectron spectroscopy (XPS) is considered as a method of choice for the determination of the elemental and chemical composition. In this work the influence of the morphology of graphene particles on the XPS results is studied and investigated as a function of X-ray energy, using conventional XPS with Al K α radiation and hard X-ray photoemission spectroscopy (HAXPES) using Cr K α radiation. Thereby, the information depth is varied between 10 and 30 nm. For this purpose, two commercial powders containing graphene nanoplatelets with lateral dimensions of either \approx 100 nm or in the micrometer range are compared. These larger ones exist as stack of graphene layers which is inspected with scanning electron microscopy. Both kinds of particles are then functionalized with either oxygen or fluorine. The size of the graphene particles is found to influence the degree of functionalization. Only the combination of XPS and HAXPES allows to detect the functionalization at the outermost surface of the particles or even of the stacks and to provide new insights into the functionalization process.

different fields like thermal conductivity,^[3] mechanical strength,^[4] or nonlinear optical properties.^[5] These exceptional properties could lead to a diverse range of new opportunities for applications,^[6,7] e.g., in electronics and optoelectronics,^[8] detection and sensing devices,^[9,10] biosystems,^[11] or chemical and environmental corrosion inhibition.^[12]

However, the commercialization of graphene is still limited, with many challenges yet to be addressed before this material can be employed in large scale applications. One reason is the lack of universal standards (documentary measurement procedures and reference materials) for both producers and users.^[13] Suppliers around the world produce “graphene” from different material feedstocks, using different processes, and then record different measurands for their products.

This situation leads to widespread confusion regarding repeatability of analytical results and thus product comparability, since the properties of any product containing graphene are closely related to the chemical and structural properties of the graphitic particles present in the powders used, e.g., number of layers within a particle, lattice vacancies, chemical functionalization, etc. Moreover, real world industrially produced products labeled as “graphene” powders are often mixtures of single layer graphene, bilayer graphene, few-layer graphene (3–10 layers) and even graphite particles with nanoscale dimensions.^[14] This has been described as the “fake graphene” issue,^[15] which is believed to be hindering graphene commercialization. First efforts were done to develop common, reliable and reproducible ways to characterize the morphological and chemical properties of the industrially produced material in order for users and producers to overcome the “what is my material?” barrier.^[16]

Thereby, the surface chemistry of the graphene flakes determined by the chemical functionalization processes plays a prominent role, because it affects significantly the dispersibility of particles in solvents and matrixes and must be optimized for embedding graphene flakes into real-world products resulting to composite materials with enhanced properties.^[17]


1. Introduction

Scientific and technological interest in graphene has been rapidly increasing in recent years due to its unique properties^[1,2] in

G. Chemello, X. Knigge, D. Ciornii, V.-D. Hodoroaba, J. Radnik
Bundesanstalt für Materialforschung und -prüfung
Unter den Eichen 44-46, 12203 Berlin, Germany
E-mail: joerg.radnik@bam.de

B. P. Reed, A. J. Pollard, C. A. Clifford
National Physical Laboratory
Hampton Road, TW11 0LW Teddington, UK

T. Howe, N. Vyas
Haydale Ltd.
Clos Fferws, Parc Hendre, Capel Hendre, SA18 3BL Ammanford, UK

 The ORCID identification number(s) for the author(s) of this article can be found under <https://doi.org/10.1002/admi.202300116>

© 2023 The Authors. Advanced Materials Interfaces published by Wiley-VCH GmbH. This is an open access article under the terms of the Creative Commons Attribution License, which permits use, distribution and reproduction in any medium, provided the original work is properly cited.

DOI: 10.1002/admi.202300116

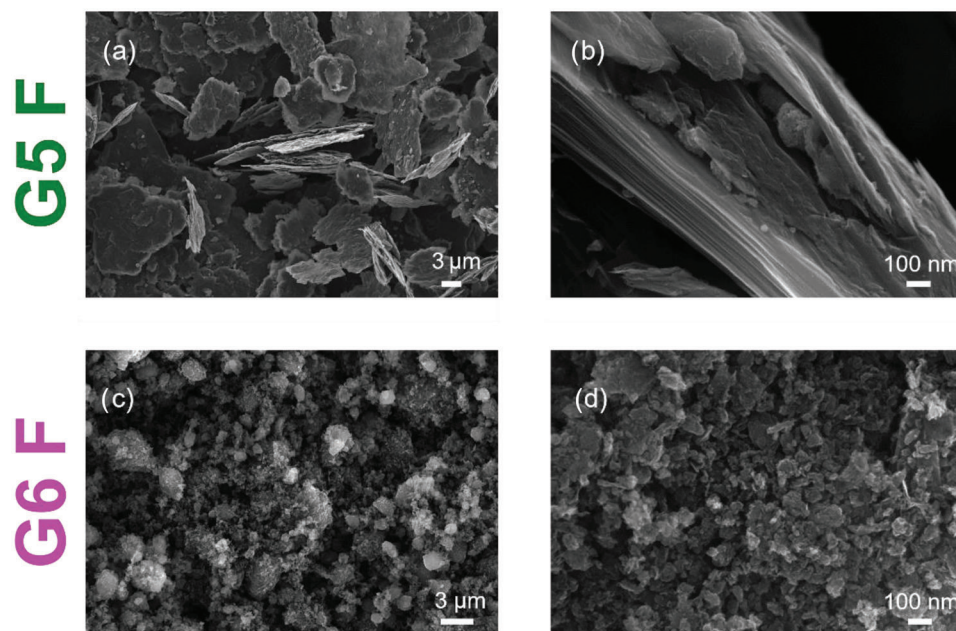


Figure 1. Representative SEM images of the fluorine-functionalized powders at different magnifications. A,b) G5F series, c,d) G6F series.

X-ray photoelectron spectroscopy (XPS) is commonly used for chemical characterization of the surface chemistry of graphene-related two-dimensional materials (GR2M) including graphene, reduced graphene oxide, graphene oxide and functionalized versions of these.^[18,19] An ISO standard for the chemical characterization of GR2Ms in powders and liquid suspensions is under development in ISO/TC 229 Nanotechnologies with XPS having a prominent role.^[20] XPS has an information depth of around 10 nm which is a similar length scale as the thickness of particles of 2D materials consisting of a few monolayers. Information depths larger than 20 nm can be obtained by using hard X-ray photoemission spectroscopy (HAXPES) with X-ray excitation energies higher than 3 keV. The higher excitation energies lead to emission of photoelectrons with a higher kinetic energy and a larger inelastic mean free path within the sample compared to conventional XPS.^[21,22] Comparison of photoelectrons of different energies coming from the same orbital allows analysis of the depth distribution of the chemical components in the sample, in a non-destructive way (e.g., without sputtering), and to note, in one instrument. Questions like the influence of adventitious carbon or the exact location of the functional groups at the surface of the graphene layers or in the bulk can be answered by the comparison of XPS with HAXPES.

In this study the chemical composition of six different commercially available powders containing graphene nanoplatelets, including oxygen and fluorine plasma-functionalized versions, were investigated using XPS and HAXPES. As shown by scanning electron microscopy (SEM) inspection, two series with different morphology of the constituent particles was found. The relationship between these different morphologies and the chemical functionalization is discussed.

2. Results and Discussion

SEM was used to investigate the particle size and morphology of the two different series of graphene materials, denominated G5 and G6 according to the naming of the provider. The type of functionalization is given after the “G5” and “G6,” with “raw” for the raw material, “O” for oxygen-functionalized materials and “F” for the fluorinated graphene. Between G5 and G6 substantially different morphologies were observed. Representative SEM images of the F-functionalized graphene are presented in **Figure 1**. Additional SEM measurements of the raw and the oxygen functionalized material showed that the functionalization process did not change the morphology of the particles, see Figures S1 and S2 (Supporting Information).

The SEM images show the G5 material consists of large and jagged particles with a size of $\approx 10\text{--}100\ \mu\text{m}$. The majority of the flakes are stacked and orientated parallel to the plane of the sample holder. A few particles are tilted which shows that this material generally consists of stacks of graphene layers with thicknesses of several 100 nm. This is the typical morphology of the G5 material as received and the stacking is not due to sample preparation. The G6 material consists of more irregular, small and rounded particles of $\approx 100\ \text{nm}$ in size. In contrast to the G5 particles, and also due to their rather isotropical shape, the G6 particles show a lack of preferential orientation. The average size of the G6 particles appears to be smaller than the stacks of graphene layers observed for G5.

X-ray diffraction (XRD) investigations of the raw and O-functionalized samples show a graphitic structure with a main reflex at $2\theta = 26.6^\circ$ and a small one at $2\theta = 54.6^\circ$ (see Figure S3, Supporting Information). An additional reflex at $2\theta = 43.3^\circ$ like the smaller reflex at $2\theta = 78.1^\circ$ was only found for the G6 samples, but it was vanished for the G5 samples. Such a behavior

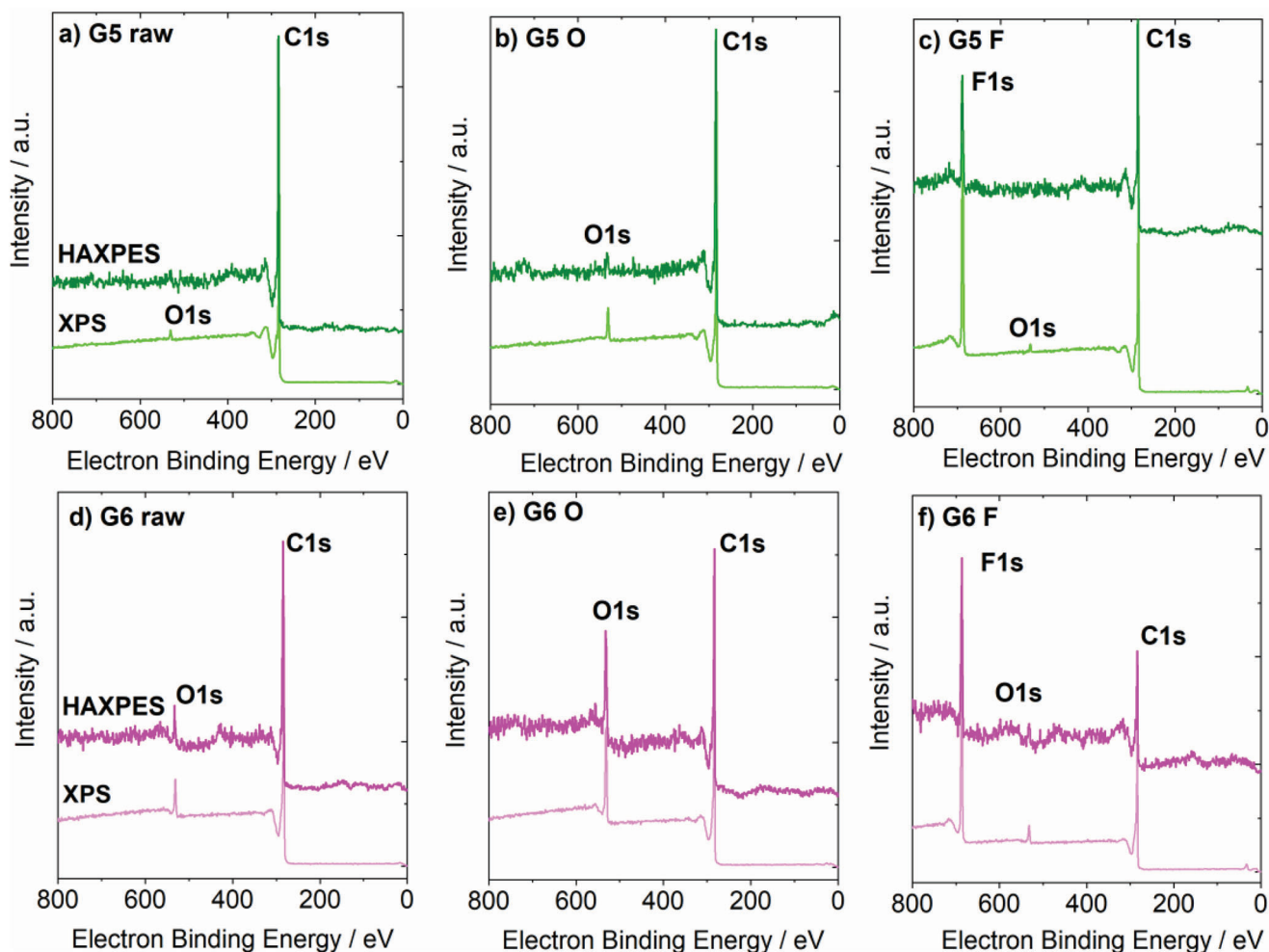


Figure 2. XPS and HAXPES spectra of the raw and functionalized graphene materials: a–c) G5 materials; d–f) G6 materials. A section between 750 and 0 eV electron binding energy is shown.

can be explained by the preferential orientation of the flakes in G5 as observed by SEM or was discussed with respect to a short-range order in stacked graphene layers.^[23] The broader halfwidth of the reflexes in the G6 samples indicates the small crystallite size in these samples and underlines the nanoscale character of the flakes.

Nitrogen gas physisorption methods have been undertaken to measure the specific surface area of the two materials. The Brunauer–Emmett–Teller (BET) equation was employed to measure the surface area from nitrogen sorption isotherms giving results of $41 \pm 2 \text{ m}^2 \text{ g}^{-1}$ for G5 and $753 \pm 8 \text{ m}^2 \text{ g}^{-1}$ for G6 powder samples.^[24]

The XPS and HAXPES spectra in **Figure 2**, compare the wide scan chemical analyses for the G5 and G6 series for unfunctionalized (raw) (a and d), oxygen- (b and e), and fluorine-functionalized (d and f) material, respectively, in the region between 0 and 800 eV. The whole spectra are shown in Figures S4 and S5 (Supporting Information). Here, a relative uncertainty between 10% (for major peaks) and 20% (for smaller peaks) was estimated for the intensity of the XPS peaks.^[25,26] The uncertainty considers the sensitivity factors as the main source of uncertainty,

the peak area determination including the background and the standard deviation corresponding to the measurements at three different points. Due to the lower cross sections of the 1s peaks for higher X-ray radiation energies, the signal-to-noise ratio for HAXPES is lower. Therefore, we estimated a higher relative uncertainty of 20–30% for the HAXPES data. For the quantitative analysis and comparison of the results between the different samples, the X/C (X = functional element) atomic ratio was calculated and shown in **Figure 3**. For the raw and oxygen-functionalized materials the O/C atomic ratio was used and for the fluorine-functionalized material the F/C ratio was used.

Two trends can be observed in the results shown in **Figure 3**. Firstly, for both the XPS and HAXPS results the atomic percentage amount of the functional element is higher for the G6 series compared to the G5 series for all measurements. This result is expected. The G6 material contains smaller particles, as shown by the SEM images and indicated by the halfwidth of the reflexes in the diffraction patterns, and thus has a larger specific surface area compared to the larger G5 particles which was shown with the former BET measurements. The plasma functionalization occurs at the surface of the particles, thus the G6 material with the

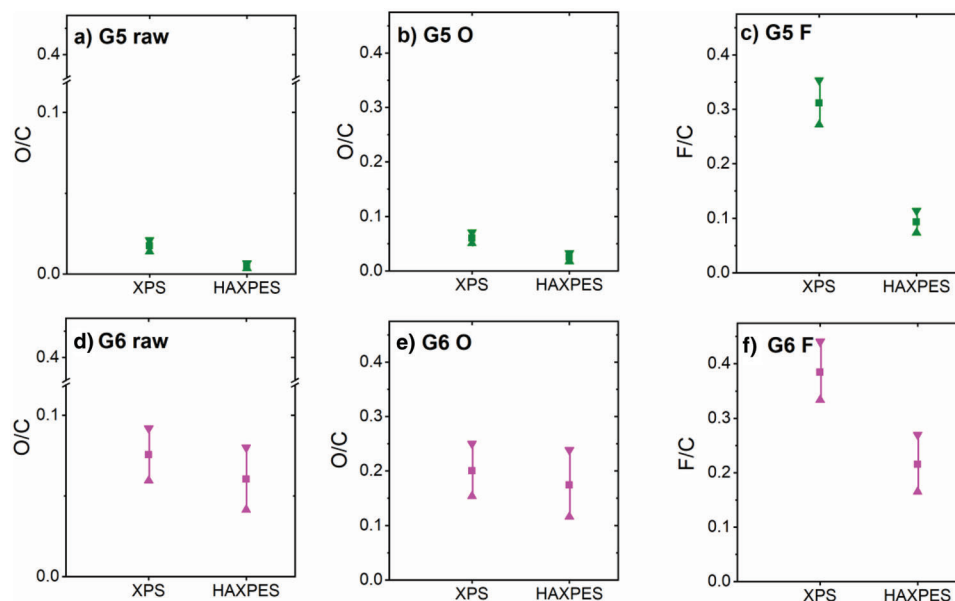


Figure 3. Comparison of the atomic ratio of functional element X (X = O or F) to C between XPS and HAXPES for all samples. The range of uncertainty is given by the maximum and the minimum values. The measured average value is the mean of this range. For the raw sample, O as the major component next to C was considered.

higher surface area has a higher ratio of the functional element X (X = O or F) to C (as the representative of the particle bulk) compared to the larger G5 particles. This ratio can be defined as degree of functionalization of the graphene.

The second trend is related to the comparison between XPS and HAXPES. For all samples, lower X/C ratios could be observed with HAXPES. This trend was reliably noted for all samples of the G5 series, even considering the estimated uncertainty. For the G6 series, such a behavior was only found for the F-functionalized graphene which has a relatively high degree of functionalization compared to the O functionalized material. For the other G6 samples only slight differences between the XPS and HAXPS results were seen which are within the range of uncertainty. The probing depth of HAXPES is around three times higher than that for XPS. This is due to higher excitation energy and herewith, the higher kinetic energy of the 1s photoelectrons. Therefore, the results can again be explained due to the functionalization occurring at the surface. The particles of the G6 samples are not preferentially orientated due to their isotropic morphology in contrast to the ones of the G5 series which present a more layer-like orientation with the larger surfaces parallel to the plane of the sample holder. The G5 particles are also significantly larger than the G6 particles. The SEM images in Figure 2 show such an arrangement. These different spatial and size arrangement of the stacks of graphene layers observed for G5 and the graphitic particles typical for G6 are shown in the schematic images of the two materials in Figure 4. The sample volume colored in red is detectable by XPS, the volume colored in red and blue is observable with HAXPES. For the G5 material, only the first outermost layers of the stack can be detected with XPS, with HAXPES additionally detecting the few layers beneath that. As discussed above, only the outermost surface layers of the stacks are functionalized and the graphene layers within the stack appear to be unfunctionalized. In contrast, for the smaller G6 particles, both XPS and HAXPES probe one to

several whole G6 particles deep. For the functionalized samples that have a lower percentage degree of functionalization like G6 O the differences are in the range of the relative uncertainty of 20–30%. Only for G6 F, which has a high degree of functionalization, differences can be observed which hint that the functionalization is mainly located on the surface of the particles.

High-resolution photoelectron spectra allowed further insights into the surface chemistry. In the C1s spectra (Figure 5) of all sample, the asymmetric peak at 284.5 eV typical for sp^2 -hybridized carbon dominates.^[27] As expected, $\pi-\pi^*$ satellite peaks around 292 eV were found which are typical for aromatic systems. Surprisingly, the satellite can be better observed with HAXPES, which hints to a relatively higher cross section for the satellite at the higher excitation energies. The percentage of C1s peaks with higher binding energy than 286 eV is higher for the G6 samples than for the G5 samples which confirms the higher degree of functionalization for this kind of samples. The most significant differences between XPS and HAXPES were observed for the fluorine functionalized samples, as expected. Furthermore, similar functional groups were found for XPS and HAXPES which exclude the presence of other functional groups within the graphene particles. The decrease of the amount of the functional elements O and F in the HAXPES spectra can be explained by the location of O and F at the outermost surface and not by the formation of other functional groups in the in the “deeper” regions of the particles. It must be noted that the halfwidth of the peaks in the HAXPES spectra are broader due to the larger linewidth of the Cr K α radiation.

For the raw graphene and oxygen-functionalized graphene alcohol- and oxo-groups can be identified from the C1s and O1s spectra (see Figures S6 and S7, Supporting Information). Whereas for the raw and oxygen-functionalized samples a similar amount of oxo ($E_B = 531.5$ eV) and alcohol groups ($E_B = 533$ eV) was observed,^[28] for the corresponding G6 sample a higher

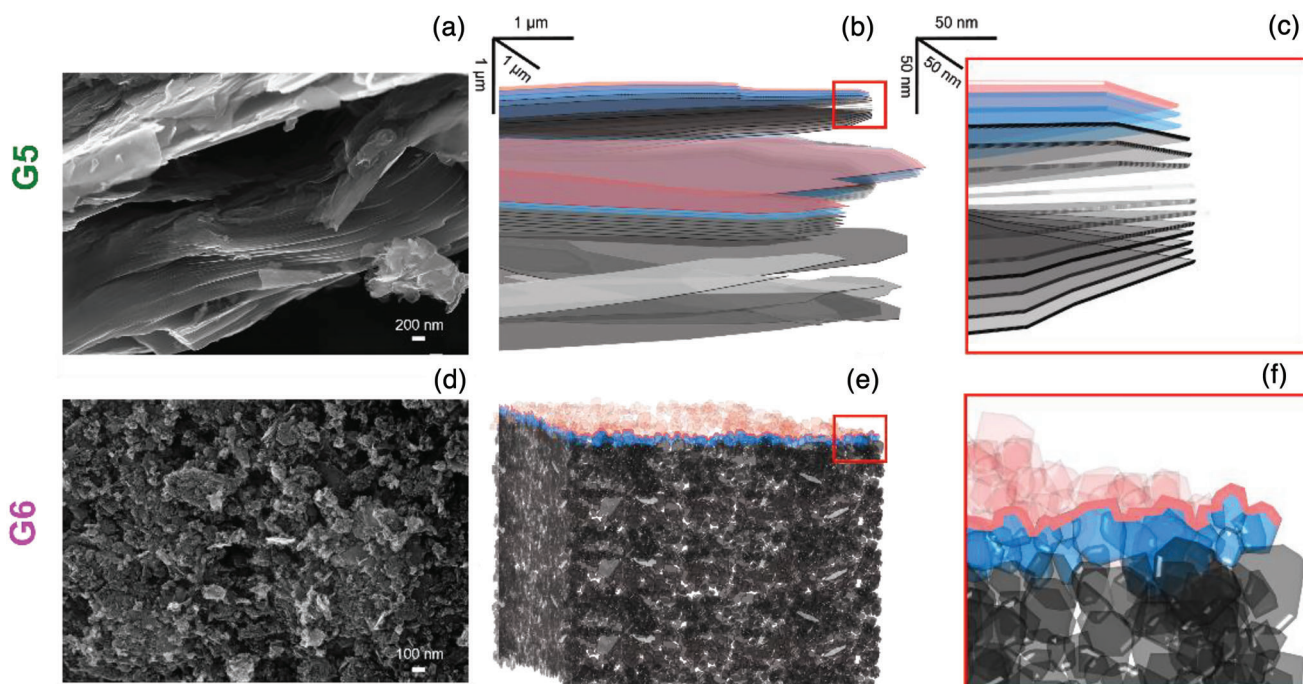


Figure 4. SEM images of a) G5 raw and d) G6 raw and scheme of the arrangement of the b,c) G5 and e,f) G6 graphene layers or particles. Details of the near-surface regions are shown in (c) and (f). The XPS information depth is marked with red, the additional HAXPES depth with blue.

amount of alcohol groups were found. For the fluor-treated samples single-fluorinated carbon atoms with a F1s binding energy of 688 eV seems to dominate. C 1s spectra hints to a small amount of carbon atoms fluorinated with more than one F atom.^[28]

3. Conclusions

XPS allows determining the degree of functionalization which is correlated with the surface area of the graphene samples: small graphitic particles of ≈ 100 nm show a higher ratio of the functional element than the stacks of large graphene layers with a size from 10 to 100 μm . In combination with HAXPES depth profiling is possible. For the stacks of graphene layer, basically only the outermost layers seem to be functionalized. The layers within the stacks are unaltered by the functionalization process. For the smaller graphitic particles, the differences between the XPS and HAXPES quantification results are not so pronounced. Only for the F-functionalized samples with a high degree of the functional element a significant higher amount of F was found with XPS than with HAXPES, but less pronounced than for the stacks of graphene layers. A substantial part of the “inner” functionalized particle surfaces can be detected with HAXPES due to larger information depth and the smaller size of the particles.

Summing up, we can conclude that we have demonstrated that XPS is a suitable method for determining the degree of functionalization of industrial graphene samples. Thereby, the morphology of the particles must be considered and correlated with the XPS results. Therefore, besides SEM, XRD, and BET results are suitable methods to obtain basic information about the morphology of the flakes.

Comparison of XPS results with HAXPES allows localizing the functional element onto/within the particles due to the different information depths. Such knowledge is crucial for a better understanding of the functionalization process of graphene, and more generally, of 2D graphene-related materials. Furthermore, such detailed material knowledge is decisive for the application of graphene nanoplatelets in different fields, like composites, inks, or sensors.

4. Experimental Section

Materials: The materials analyzed in this study are industrially produced and consist of plasma-functionalized graphene particles provided as powders. Two different series of samples, labeled here as G5 and G6, were used, the two different series having different particle morphologies. Within each series, two types of chemical functionalization were undertaken: oxygen-functionalized (O) and fluorine-functionalized (F). The unfunctionalized (raw) starting materials were also analyzed. The functionalized particles were produced by Haydale Ltd. (Ammanford, UK) using a plasma treatment described in detail elsewhere.^[29] Briefly, commercially available graphitic nanoplatelets were placed in a patented reactor barrel and loaded into a HDPlas plasma reactor. Feed gas was introduced into a low-pressure chamber where it was energized and ionized to create a plasma. Gas flow and pressure were regulated by a mass flow controller and a metered vacuum source. The reactor barrel both acted as a counter-electrode and rotated around the central electrode to facilitate mixing. The reaction process integrates pre-treatment and post-treatment to ensure homogeneity of the starting material and final product.

Hard-Energy X-Ray and Conventional X-Ray Photoemission Spectroscopy: A sample holder with a 5 mm recess of 1 mm depth was filled with the powder, then the surface was levelled with a spatula and slightly pressed to create an evenly flat and regular sample surface parallel to the sample holder surface, see **Figure 6**. This process removes the outer portion of

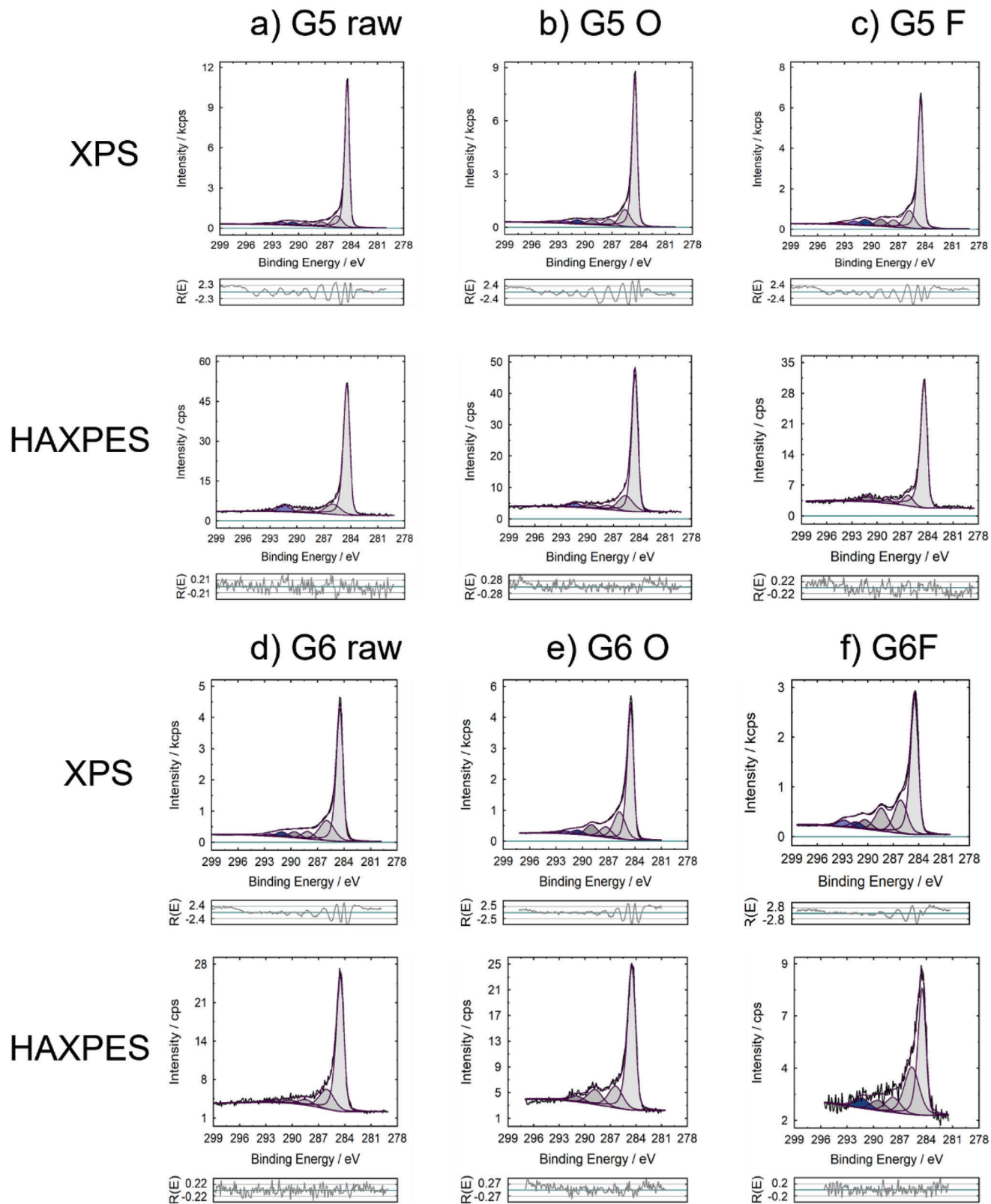


Figure 5. XPS and HAXPES C1s high-resolution spectra of a) G5 raw, b) G5 O, c) G5 F, d) G6 raw, e) G6 O and G6 raw, and f) G6 F.

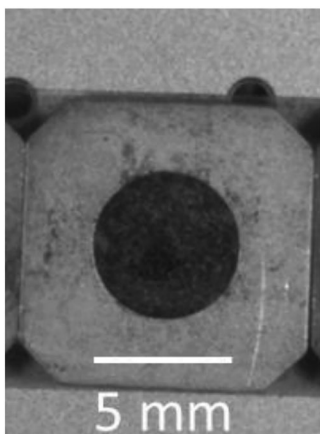


Figure 6. Optical image of the XPS/HAXPES sample holder showing the 5 mm diameter recess filled with powder.

the material, thus avoiding alteration to the powder structure and minimizing effects on the particle morphology by the sample preparation. Prior to measurement, the samples were stored in a desiccator under vacuum at a pressure of 100 Pa for two days to shorten the time needed for pumping down to ultrahigh vacuum (UHV) inside the instrument chamber. The sample holders were fixed with a double adhesive carbon tape on the platen provided by the manufacturer.

XPS and HAXPES measurements were performed using a lab-based ULVAC-PHI “Quantex” spectrometer (Chanhasen, USA), that is equipped with two X-ray sources: a monochromatic Al $K\alpha$ -source at 1486.6 eV for XPS and a monochromatic Cr $K\alpha$ -source at 5414.8 eV for HAXPES. With this spectrometer, it was possible to perform XPS and HAXPES measurements at the exact same location on the sample. The spot size of the X-ray beam can be adjusted and was set to 100 μm for this work. Photoelectrons were collected at an emission angle of 45° for both XPS and HAXPES. The Al $K\alpha$ -source was situated normal to the sample, the incident angle of the Cr $K\alpha$ -source was 22°. The pressure in the sample chamber was kept below 10⁻⁶ Pa during the measurements. The measurements were performed at three different areas of the samples. Low energy electrons and Ar⁺ ions were used for charge neutralization. The spectra were referenced to the C1s binding energy of 284.5 eV.

The XPS and HAXPES spectra were collected as survey spectra with a step size of 1 eV at a pass energy of 280 eV and a time per step of 200 ms. The measurements were repeated with 2 sweeps for XPS at an X-ray power of 25 W at 15 kV. Here the binding energy range selected was from 0 to 1100 eV. For the HAXPES survey spectra, the repetition rate was set to 10 sweeps, at an X-ray power of 50 W at 20 kV. The selected binding energy range was from 0 to 5000 eV.

The high-resolution spectra were measured with a pass energy of 54 eV and a step size of 0.1 eV for XPS; for HAXPES a pass energy of 69 eV and a step size of 0.125 eV were chosen. The following sequence for the measurement was used: 1) XPS survey spectra, 2) HAXPES survey spectra, 3) XPS high resolution spectra, and 4) HAXPES high resolution spectra.

For the quantification of the atomic concentration, the PHI MultiPak Software Version 9.9.1 was used, with relative empirical sensitivity factors provided by the manufacturer. The binding energy scale was calibrated following a PHI procedure that uses ISO 15472 binding energy data.^[30] The intensity was calibrated with the PHI MultiPak software following a procedure introduced by Seah.^[31] A Shirley background was used.

For peak fitting Unifit 2022 was used with the sum Gaussian–Lorentzian curves and a modified Tougaard background.^[32,33]

Scanning Electron Microscopy: The morphology imaging of the powders was carried out using a SEM instrument of type Zeiss Supra 40 (Oberkochen, Germany), with a Schottky field emitter and a secondary electron InLens detector, to obtain high-resolution images of the powder samples surface. The SEM imaging was performed on a different sample

batch prepared in exactly the same way as for the XPS and HAXPES samples.

Powder X-Ray Diffraction: For the recording of the data a D8 Advance Diffractometer (Bruker AXS, Karlsruhe, Germany) equipped with an energy dispersive LynxEye XE-T detector was used. The powder specimens were prepared in zero background sample holders. Measurements were performed in Bragg–Brentano Geometry with a Copper X-Ray source with a wavelength of 1.54178 Å without monochromator and an X-ray tube power of 40 kV times 40 mA. As measurement parameter the following were chosen: 3–80° 2 θ measurement range, 0.02° step size, 1 s measurement time per step and 1 h total measurement time.

Supporting Information

Supporting Information is available from the Wiley Online Library or from the author.

Acknowledgements

The authors give thanks to Sigrid Benemann for carrying out the SEM measurements and Dominik Al-Sabbagh for the XRD measurements (both BAM). David Cant, Alex Shard, and Caterina Minelli (all NPL) are acknowledged for their helpful comments. The commercial powders were sourced and functionalized by Haydale Ltd. (UK). This project “Standardisation of structural and chemical properties of graphene” (ISO-G-SCoPe) was received funding from the EMPIR programme co-financed by the Participating States and from the European Union’s Horizon 2020 research and innovation programme under Grant agreement No. 19NRM04 ISO-G-SCoPe.

Open access funding enabled and organized by Projekt DEAL.

Conflict of Interest

The authors declare no conflict of interest.

Data Availability Statement

The data that support the findings of this study are available under <https://doi.org/10.5281/zenodo.7956498>.

Keywords

fluorine, functionalized graphene, hard X-ray photoelectron spectroscopy, oxygen, raw, X-ray photoelectron spectroscopy

Received: February 7, 2023

Revised: May 5, 2023

Published online:

- [1] X. Huang, Z. Yin, S. Wu, X. Qi, Q. He, Q. Zhang, Q. Yan, F. Boey, H. Zhang, *Small* **2011**, 7, 1876.
- [2] G. Yang, L. Li, W. B. Lee, M. C. Ng, *Sci. Technol. Adv. Mater.* **2017**, 19, 613.
- [3] S. Ghosh, I. Calizo, D. Teweldebrhan, E. P. Pokatilov, D. L. Nika, A. A. Balandin, W. Bao, F. Miao, C. N. Lau, *Appl. Phys. Lett.* **2008**, 92, 151911.
- [4] C. Lee, X. Wei, J. W. Kysar, J. Hone, *Science* **2008**, 321, 385.
- [5] Z. B. Liu, X. L. Zhang, X. Q. Yan, Y. S. Chen, J. G. Tian, *Chin. Sci. Bull.* **2012**, 57, 2971.

- [6] P. Walimbe, M. Chaudhari, *Mater. Today Sustain.* **2019**, *6*, 100026.
- [7] J. Phiri, P. Gane, T. C. Maloney, *Mater. Sci. Eng. B* **2017**, *215*, 9.
- [8] M. Sang, J. Shin, K. Kim, K. J. Yu, *Nanomaterials* **2019**, *9*, 374.
- [9] Q. Zheng, J. Lee, X. Shen, X. Chen, J.-K. Kim, *Mater. Today* **2020**, *36*, 158.
- [10] E. J. Legge, M. M. Ali, H. Y. Abbasi, B. P. Reed, B. Brennan, L. Matjačić, Z. Tehrani, V. Stolojan, S. R. P. Silva, O. J. Guy, A. J. Pollard, *J. Chem. Phys.* **2021**, *155*, 174703.
- [11] N. Lu, L. Wang, M. Lv, Z. Tang, C. Fan, *Nano Res.* **2018**, *12*, 247.
- [12] F. Perreault, A. Fonseca De Faria, M. Elimelech, *Chem. Soc. Rev.* **2015**, *44*, 5861.
- [13] C. A. Clifford, E. H. Martins Ferreira, T. Fujimoto, J. Herrmann, A. R. Hight Walker, D. Koltsov, C. Punckt, L. Ren, G. J. Smallwood, A. J. Pollard, *Nat. Rev. Phys.* **2021**, *3*, 233.
- [14] A. J. Pollard, C. A. Clifford, *J. Mater. Sci.* **2017**, *52*, 13685.
- [15] P. Bøggild, *Nature* **2018**, *562*, 502.
- [16] ISO/TS 21356-1:2021: Nanotechnologies – Structural characterization of graphene – Part 1: Graphene from powders and dispersion, Geneva, **2021**.
- [17] M. Naebe, J. Wang, A. Amini, H. Khayyam, N. Hameed, L. H. Li, Y. Chen, B. Fox, *Stem Cells Int.* **2014**, *4*, 4375.
- [18] R. Al-Gaashani, A. Najjar, Y. Zakaria, S. Mansour, M. A. Atieh, *Ceram. Int.* **2019**, *45*, 14439.
- [19] F. Priante, M. Salim, L. Ottaviano, F. Perrozzi, *Nanotechnology* **2018**, *29*, 075704.
- [20] ISO. ISO/AWI TS 23359 Nanotechnologies — Chemical characterization of graphene in in powders and suspensions. <https://www.iso.org/standard/83450.html?browse=tc> (accessed: January **2023**).
- [21] C. J. Powell, A. Jablonski, *Nucl. Instrum. Methods Phys. Res. A* **2009**, *601*, 54.
- [22] C. J. Powell, A. Jablonski, I. S. Tilinin, S. Tanuma, D. R. Penn, *J. Electron Spectrosc. Relat. Phenom.* **1999**, *98–99*, 1.
- [23] L. Stobinski, B. Lesiak*, A. Malolepszy, M. Mazurkiewicz, B. Mierzwa, J. Zemek, P. Jiricek, I. Bieloshapka, *J. Electron Spectrosc. Relat. Phenom.* **2014**, *195*, 145.
- [24] B. P. Reed, S. Marchesini, G. Chemello, D. J. Morgan, C. A. Clifford, J. Radnik, A. J. Pollard, *Carbon* **2023**, *211*, 118054.
- [25] C. R. Brundle, B. V. Crist, *J. Vac. Sci. Technol. A* **2020**, *38*, 041001.
- [26] J. Radnik, R. Kersting, B. Hagenhoff, F. Bennet, D. Ciornii, P. Nymark, R. Grafström, V. D. Hodoroaba, *Nanomaterials* **2021**, *11*, 639.
- [27] M. C. Biesinger, *Appl. Surf. Sci.* **2022**, *597*, 153681.
- [28] G. Beamson, D. Briggs: *High Resolution XPS of Organic Polymers – The Scienta ESCA300 Database*, Wiley Interscience, New York **1992**.
- [29] N. Kumar, S. Marchesini, T. Howe, L. Edwards, B. Brennan, A. J. Pollard, *J. Chem. Phys.* **2020**, *153*, 184708.
- [30] ISO 15472:2010 Surface chemical analysis — X-ray photoelectron spectrometers — Calibration of energy scales. Geneva, **2010**.
- [31] M. P. Seah, *J. Electron Spectrosc. Relat. Phenom.* **1995**, *71*, 191.
- [32] R. Hesse, P. Streubel, R. Szargan, *Surf. Interface Anal.* **2007**, *39*, 381.
- [33] R. Hesse, R. Denecke, *Surf. Interface Anal.* **2011**, *43*, 1514.